



# Journal of Applied Sciences

ISSN 1812-5654

**science**  
alert

**ANSI***net*  
an open access publisher  
<http://ansinet.com>

## Characterization of Elliptically Polarized Light and Rotation Angle of PBS in Three-Longitudinal-Mode Laser Interferometer Using the Jones Matrices

Saeed Olyaei and Shahram Mohammad Nejad  
Department of Electrical Engineering, Iran University of Science and Technology,  
Narmak, 16846, Tehran, Iran

**Abstract:** In this study, the periodic nonlinearities resulting from ellipticity of polarized light and rotation angle of Polarizing Beam Splitter (PBS) with respect to the laser axis are presented. The nonlinearity in the three-longitudinal-mode laser interferometer is mathematically modeled using the Jones matrices. Based on the nonlinearity compensation for two-color interferometers, a new optical setup and signal conditioner circuit is also designed. Using the nonlinearity compensation setup, the peak-to-peak nonlinearity of 2.64 nm due to two-elliptically polarized modes in combination with rotation angle of polarizing beam splitter is successfully reached 26 pm.

**Key words:** Jones matrix, laser interferometer, nonlinearity, elliptically polarized light

### INTRODUCTION

This study presents a new nonlinearity compensator for error reduction in three-longitudinal-mode interferometers. The nonlinearity reduction in the three-longitudinal-mode interferometer can effectively increase the nanometric displacement measurement accuracy. Laser interferometers are being widely used as instrument systems for small displacement measurement with sub-nanometric uncertainty. Two-color interferometers are commercially used for increasing the range of unambiguity. But the displacement measurement accuracy can be improved by replacing the two-color source by three-longitudinal-mode laser. A sub-nanometer heterodyne interferometric system using three-longitudinal-mode He-Ne laser is presented by Yokoyama *et al.* (2001) and then by utilizing a proper configuration, the maximum measurable velocity is enhanced (Yokoyama *et al.*, 2005).

The displacement accuracy is limited by many factors such as laser frequency instability, uncertainty of the refractive index determination, phase detection error and thermal instabilities (Yim *et al.*, 2000; Kim and Kim, 2004; Olyaei and Mohammad Nejad, 2007a). The optical setup can also effectively decrease the displacement accuracy. The optical deviations can be divided into two main groups' namely imperfect alignment and non-ideal polarized beams. These phenomena produce the periodic nonlinearity error that is modeled by Cosijns *et al.* (2002) for two-mode interferometer. However, imperfect

alignment of optical components and non-ideal polarized light emerging from the laser head can limit the displacement measurement accuracy of the laser interferometers.

The modeling of polarization properties can be done by plane wave or matrix methods. Based on the Jones calculus, matrix methods are suited to modeling of polarization sensitive systems. In fact the Jones calculus is a powerful and simple method for modeling optical systems involving polarized modes.

In the present study, we characterized and mathematically modeled the most important optical deviations including ellipticity of polarized modes and rotation angle of polarizing beam splitter in three-longitudinal-mode heterodyne interferometer by using the Jones matrices of the optical components. In addition, we improved the system performance by designing an optical setup and a signal conditioner circuit in the measurement arm. The results confirm that the periodic nonlinearities are strongly reduced.

### MATERIALS AND METHODS

A three-longitudinal-mode heterodyne interferometer similar to current commercial interferometric systems consists of two arms namely base and measurement (Olyaei and Mohammad Nejad, 2007b). Also measurement arm includes reference and target paths. The measurement beam is split into target and reference beams by the polarizing beam splitter. Ideally, the side and central

modes are directed towards the reference and target corner cube prisms, respectively. When a rotation angle of polarizing beam splitter with respect to the laser head or elliptically polarized modes appears, there will be leakage of modes.

According to Fig. 1, the ellipticity of side and central modes are denoted by  $\delta_{e_r}$  and  $\delta_{e_s}$ , respectively. Therefore, the electrical fields of three optical frequencies are respectively given by:

$$\vec{E}_1 = \begin{bmatrix} \cos \delta_{e_r} \\ -j \sin \delta_{e_r} \end{bmatrix} e^{jx_1} \quad (1)$$

$$\vec{E}_2 = \begin{bmatrix} -j \sin \delta_{e_s} \\ \cos \delta_{e_s} \end{bmatrix} e^{jx_2} \quad (2)$$

$$\vec{E}_3 = \begin{bmatrix} \cos \delta_{e_r} \\ -j \sin \delta_{e_r} \end{bmatrix} e^{jx_3} \quad (3)$$

where,  $x_i = 2\pi\nu_i t + \varphi_{0i}$ ,  $i = 1, 2, 3$  are the optical frequencies and  $\varphi_{0i}$  are the initial phases. By Jones calculus, the Jones vector of the reference electrical field is obtained as

$$\vec{E}_r = \text{PBS}_r \cdot \text{CCP}_r \cdot \text{PBS}_r \cdot \left( \sum_{i=1}^3 \vec{E}_i \right) \quad (4)$$

where,  $\text{PBS}_r$  and  $\text{CCP}_r$  are the Jones matrices of the polarizing beam splitter and reference corner cube prism for reference beam, respectively, shown in Fig. 2. It is assumed that the optical axis of polarizing beam splitter is aligned properly compared to the laser head. These matrices can be described as:

$$\text{PBS}_r = \begin{bmatrix} 1 & 0 \\ 0 & 0 \end{bmatrix} \quad (5)$$

$$\text{CCP}_r = \begin{bmatrix} -1 & 0 \\ 0 & -1 \end{bmatrix} \quad (6)$$

Similar to the reference path, the Jones vector of the target electrical field is given by:

$$\vec{E}_t = \text{PBS}_t \cdot \text{CCP}_t \cdot \text{PBS}_t \cdot \left( \sum_{i=1}^3 \vec{E}_i \right) \quad (7)$$

where:

$$\text{PBS}_t = \begin{bmatrix} 0 & 0 \\ 0 & 1 \end{bmatrix} \quad (8)$$

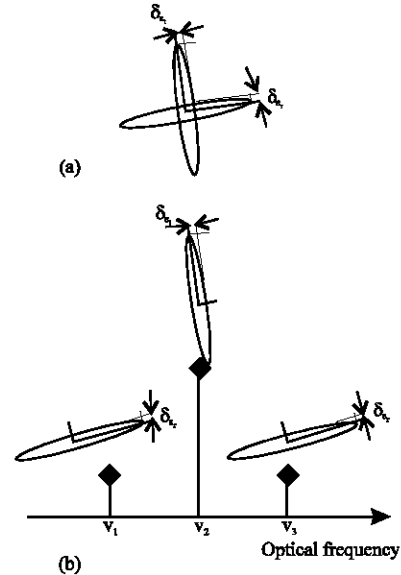


Fig. 1: Schematic representation of (a) the ellipticity of orthogonal polarized modes and (b) the position of three-longitudinal-mode in the gain profile

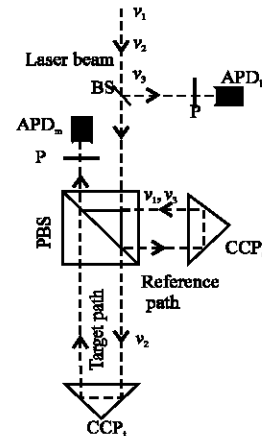


Fig. 2: The optical setup of the three-longitudinal-mode laser interferometer

$$\text{CCP}_t = \begin{bmatrix} -\exp(j\Delta\Phi) & 0 \\ 0 & -\exp(j\Delta\Phi) \end{bmatrix} \quad (9)$$

where,  $\Delta\Phi = 4n\pi\Delta d/\lambda$ ,  $n$  is the refractive index,  $\lambda$  is the central wavelength and  $\Delta d$  is the optical path difference between two paths. The total electric field can be obtained by summing the reference and target fields.

$$\vec{E}_{BS} = \vec{E}_r + \vec{E}_t \quad (10)$$

The Jones vector of the electrical field incident on the ideal polarizer with  $45^\circ$  orientation is given as:

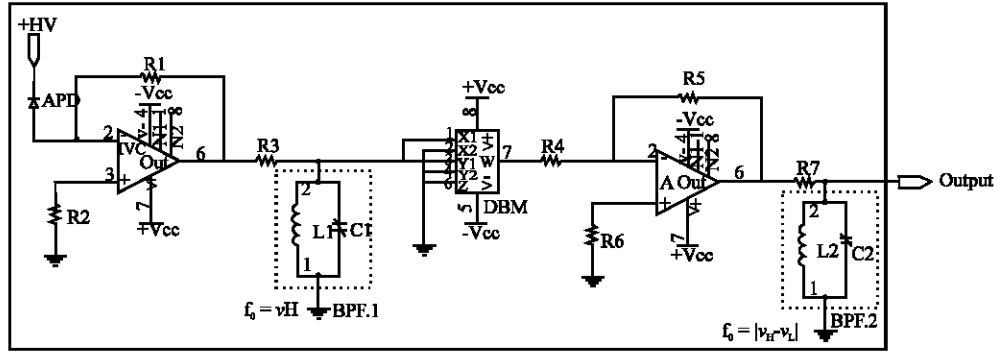


Fig. 3: The schematic diagram of analog signal conditioner for base and measurement arms

$$\vec{E}_p = P \cdot \vec{E}_{BS} = \frac{1}{2} \begin{bmatrix} 1 & 1 \\ 1 & 1 \end{bmatrix} \vec{E}_{BS} \quad (11)$$

The wave intensity can be expressed as the product of the electrical field and its complex conjugate. As a result, the photocurrent of the measurement avalanche photodiode,  $I_{pAPD,m}$ , is

$$I_{pAPD,m} = \vec{E}_p^* \vec{E}_p \quad (12)$$

where,  $\vec{E}_p^*$  is the complex conjugate of the electrical field. Substitution of Eq. 11 into Eq. 12 gives a quite complex equation. But the optical frequencies are eliminated by the measurement avalanche photodiode (APDm). Furthermore, in the signal conditioner circuit a Band Pass Filter (BPF) is used, as shown in Fig. 3. DC component and high order frequencies (e.g.,  $\nu_1 + \nu_2$ ,  $2\nu_2$ ,  $\nu_2 + 2\nu_3$ ) are eliminated and primary beat frequencies including  $\nu_2 - \nu_1$  and  $\nu_3 - \nu_2$  remain. The measurement photocurrent described in Eq. 12 is converted to voltage signal that can be simplified as:

$$V_{BPF_m} \propto a_1 (\cos(x_L - \Delta\Phi) + \cos(x_H + \Delta\Phi)) + a_2 (\cos(x_L + \Delta\Phi) + \cos(x_H - \Delta\Phi)) + a_3 (\sin x_L - \sin x_H) \quad (13)$$

where,  $x_L = 2\pi(\nu_2 - \nu_1)t + (\varphi_{02} - \varphi_{01})$  and  $x_H = 2\pi(\nu_3 - \nu_2)t + (\varphi_{03} - \varphi_{02})$  are corresponding to the lower and higher intermode beat frequencies, respectively. The constant factors in Eq. 13 are obtained as

$$a_1 = \sin \delta_{e_1} \sin \delta_{e_2} \quad (14)$$

$$a_2 = \cos \delta_{e_1} \cos \delta_{e_2} \quad (15)$$

$$a_3 = \sin(\delta_{e_1} - \delta_{e_2}) \quad (16)$$

The signal is led to a Double-Balanced Mixer (DBM) and then is filtered. Therefore the secondary beat frequency,  $x_0 = |x_H - x_L|$ , is extracted. The normalized measurement signal is:

$$V_m = (2a_1 a_2 + a_3^2) \cos x_0 - 2a_1 a_3 \sin(x_0 - \Delta\Phi) - 2a_2 a_3 \sin(x_0 + \Delta\Phi) + a_1^2 \cos(x_0 - 2\Delta\Phi) + a_2^2 \cos(x_0 + 2\Delta\Phi) \quad (17)$$

On the other hand, a similar signal conditioner is used in the base arm. Hence, the normalized base signal is given by:

$$V_b = A \cos x_0 \quad (18)$$

For extraction of the phase nonlinearity, Eq. 17 must be rewritten as:

$$V_m = A \cos(x_0 - 2\Delta\Phi + \Phi_{nl}) \quad (19)$$

where:

$$\Phi_{nl} = -\arctan \frac{(2a_1 a_2 - a_3^2) \sin 2\Delta\Phi + 2a_2 a_3 \cos \Delta\Phi + 2a_1 a_3 \cos 3\Delta\Phi + a_1^2 \sin 4\Delta\Phi}{-(2a_1 a_2 - a_3^2) \cos 2\Delta\Phi + 2a_2 a_3 \sin \Delta\Phi + 2a_1 a_3 \sin 3\Delta\Phi - a_2^2 - a_1^2 \cos 4\Delta\Phi} \quad (20)$$

Also interfering of three modes on the base avalanche photodiode produces offset phase error. This error can be obtained by substitution of zero for  $\Delta\Phi$  in Eq. 20 as:

$$\Phi_{off} = -\arctan \frac{2a_3(a_1 + a_2)}{(2a_1 a_2 - a_3^2) + a_2^2 + a_1^2} \quad (21)$$

For characterization of rotation angle of polarizing beam splitter, we assume that the polarization of modes is perfectly linear,  $\delta_{ct} = \delta_{cr} = 0$  therefore

$$\vec{E}_1 = \begin{bmatrix} 1 \\ 0 \end{bmatrix} e^{ix_1} \quad (22)$$

$$\vec{E}_2 = \begin{bmatrix} 0 \\ 1 \end{bmatrix} e^{ix_2} \quad (23)$$

$$\vec{E}_3 = \begin{bmatrix} 1 \\ 0 \end{bmatrix} e^{ix_3} \quad (24)$$

$$\vec{E}_r = \begin{bmatrix} -\cos^2 \alpha \\ -\sin \alpha \cos \alpha \end{bmatrix} (e^{ix_1} + e^{ix_3}) + \begin{bmatrix} -\sin \alpha \cos \alpha \\ -\sin^2 \alpha \end{bmatrix} e^{ix_2} \quad (28)$$

$$\vec{E}_t = \begin{bmatrix} -\sin^2 \alpha \\ \sin \alpha \cos \alpha \end{bmatrix} (e^{j(x_1+\Delta\Phi)} + e^{j(x_3+\Delta\Phi)}) + \begin{bmatrix} \sin \alpha \cos \alpha \\ -\cos^2 \alpha \end{bmatrix} e^{j(x_2+\Delta\Phi)}$$

and instead of that a rotation angle of polarizing beam splitter with respect to the laser axis is considered and denoted by  $\alpha$ . In this case the polarizing beam splitter matrices for target and reference beams are respectively taken as

$$PBS_t = \begin{bmatrix} \cos \alpha & -\sin \alpha \\ \sin \alpha & \cos \alpha \end{bmatrix} \begin{bmatrix} 0 & 0 \\ 0 & 1 \end{bmatrix} \begin{bmatrix} \cos \alpha & \sin \alpha \\ -\sin \alpha & \cos \alpha \end{bmatrix} \quad (25)$$

$$PBS_r = \begin{bmatrix} \cos \alpha & -\sin \alpha \\ \sin \alpha & \cos \alpha \end{bmatrix} \begin{bmatrix} 1 & 0 \\ 0 & 0 \end{bmatrix} \begin{bmatrix} \cos \alpha & \sin \alpha \\ -\sin \alpha & \cos \alpha \end{bmatrix} \quad (26)$$

and for the polarizer matrix,

$$P = \begin{bmatrix} \cos^2(\frac{\pi}{4} + \alpha) & \cos(\frac{\pi}{4} + \alpha)\sin(\frac{\pi}{4} + \alpha) \\ \cos(\frac{\pi}{4} + \alpha)\sin(\frac{\pi}{4} + \alpha) & \sin^2(\frac{\pi}{4} + \alpha) \end{bmatrix} \quad (27)$$

The reference and target electrical fields are calculated by substitution of above matrices in Eq. 4 and 7 as:

Based on the comprehensive study on the nonlinearities which has been characterized and simulated in the Optoelectronic and Laser Laboratory of IUST, the phase nonlinearity resulting from rotation angle of PBS with respect to the laser head can be given by

$$\Phi_{nl} = -\arctan\left(\frac{N}{F}\right) \quad (30)$$

$$N = -\sin^4 \alpha \sin 4\Delta\Phi + 2\sin^2 \alpha \cos^2 \alpha \sin 2\Delta\Phi$$

$$F = \sin^4 \alpha \cos 4\Delta\Phi + \cos^4 \alpha - 2\sin^2 \alpha \cos^2 \alpha \cos 2\Delta\Phi$$

**RESULTS AND DISCUSSION**

Earlier, the phase nonlinearity resulting from ellipticity of orthogonal polarized modes and rotation angle of PBS are modeled. Figure 4 shows the periodic nonlinearity due to the ellipticity of polarized modes in terms of the nanometric displacement. As shown in Fig. 4, the first order or second order nonlinearity can be

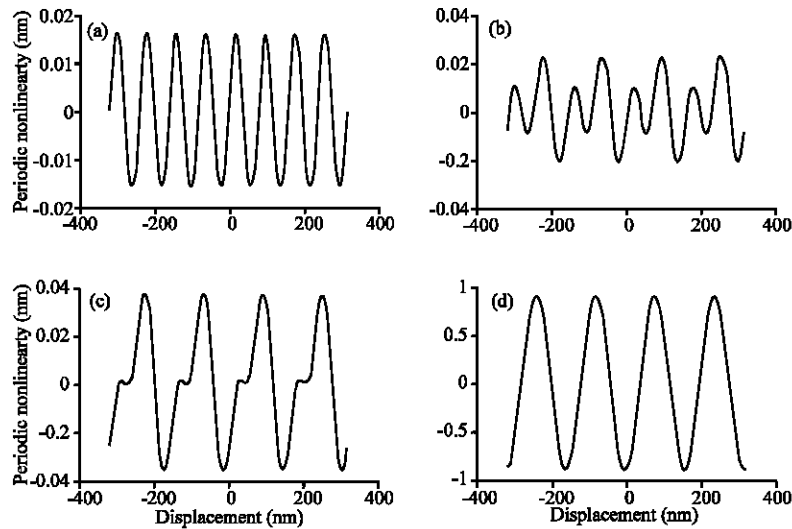


Fig. 4: The periodic nonlinearity resulting from ellipticity of polarized modes in terms of the nanometric displacement,  $\delta_{e_1} = 1^\circ$ , (a)  $\delta_{e_1} = 1^\circ$ , (b)  $\delta_{e_1} = 0.99^\circ$ , (c)  $\delta_{e_1} = 0.97^\circ$  and (d)  $\delta_{e_1} = 0$

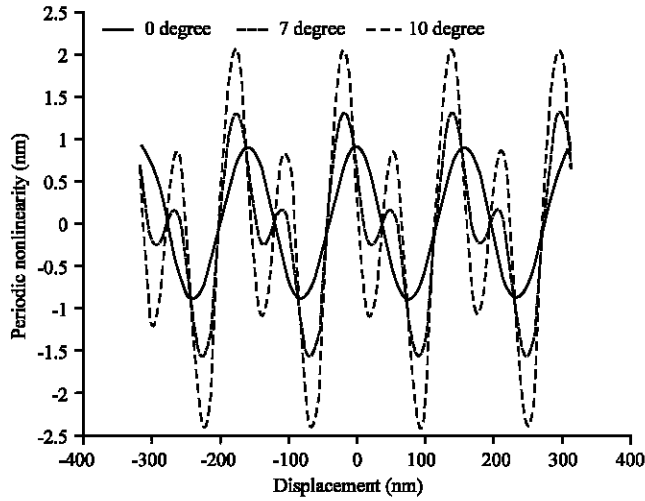


Fig. 5: The periodic nonlinearity resulting from one-elliptically polarized modes ( $\delta_{e_1} = 1^\circ, \delta_{e_2} = 0$ ) in combination with the rotation angle of polarizing beam splitter

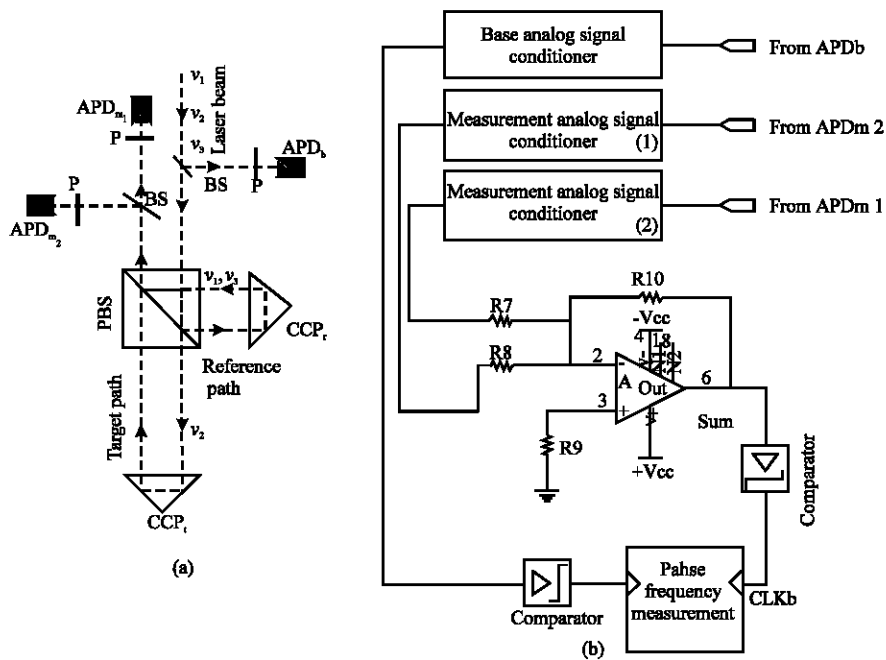


Fig. 6: The designed system for nonlinearity compensation. (a) The optical setup and (b) signal conditioner

produced. If  $\delta_{e_1} \neq \delta_{e_2}$ , the first order nonlinearity (Fig. 4d) and in other cases ( $\delta_{e_1} \cong \delta_{e_2}$ ), the second order nonlinearity appears. The rotation angle of polarizing beam splitter effect in combination with the one-ellipticity of polarized modes is shown in Fig. 5. This deviation causes to increase the peak-to-peak of the second order periodic nonlinearity.

Based on the nonlinearity compensation for two-mode interferometer presented by Hou and Wilkening (1992), we design an optical setup and a signal

conditioner for nonlinearity compensation, as shown in Fig. 6. In the measurement arm, two linear polarizers oriented at  $+45^\circ$  and  $-45^\circ$  and two avalanche photodiodes are used. The average signal of two photocurrents is produced by the signal conditioner circuit. As a result, the peak-to-peak nonlinearity is considerably decreased (Fig. 7). The peak-to-peak nonlinearity of 2.64 nm is result of the two photocurrents which by nonlinearity compensation, it is reached 26 pm.

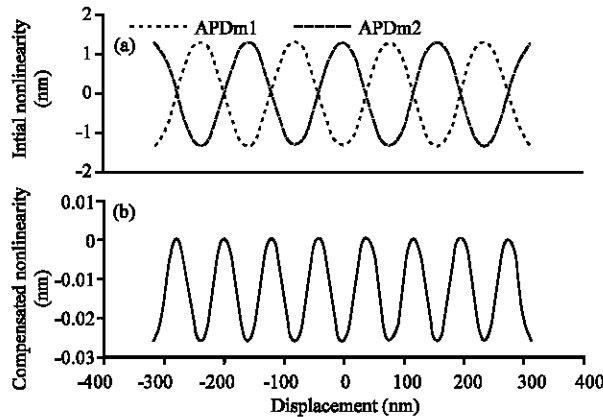


Fig. 7: The periodic nonlinearity in terms of the nanometric displacement, (a) initial nonlinearities and (b) compensated nonlinearity,  $\alpha = 1.7^\circ$ ,  $\delta_a = 1^\circ$ ,  $\delta_a = -0.5^\circ$

**CONCLUSIONS**

In this study, the periodic nonlinearities resulting from ellipticity of orthogonal polarized modes and rotation angle of polarizing beam splitter in the three-longitudinal-mode laser interferometer have been modeled. For nonlinearity modeling, the Jones matrices are used. The displacement error depends on the ellipticity and rotation angle can appear as first or second order nonlinearities. Also, an optical configuration and electronic signal conditioner are designed for nonlinearity compensation. Using this system, the periodic nonlinearity considerably decreased.

**REFERENCES**

Cosijns, S.J., H. Haitjema and P.H. Schellekens, 2002. Modeling and verifying non-linearities in heterodyne displacement interferometry. *Precision Eng.*, 26: 448-455.

Hou, W. and G. Wilkening, 1992. Investigation and compensation of the nonlinearity of heterodyne interferometers. *Prec. Eng.*, 14: 91-98.

Kim, M. and S. Kim, 2004. Two-way frequency-conversion phase measurement for high-speed and high-resolution heterodyne interferometry. *Meas. Sci. Technol.*, 15: 2341-2348.

Olyaei, S. and S. Mohammad Nejad, 2007a. A new design of frequency stabilization system based on the frequency pulling and power-balanced methods. In: *Proceedings of the 13th Iranian Annual Conference on Optics and Photonics*. The Physical Society of Iran. Iran Telecommunication Research Center (ITRC), Tehran, pp: 117-123,

Olyaei, S. and S. Mohammad Nejad, 2007b. Nonlinearity and frequency-path modeling of three-longitudinal-mode nanometric displacement measurement system. *IET Optoelectronics* (In Press).

Yim, N., C. Eom and S. Kim, 2000. Dual mode phase measurement for optical heterodyne interferometry. *Meas. Sci. Technol.*, 11: 1131-1137.

Yokoyama, T., T. Araki, S. Yokoyama and N. Suzuki, 2001. A subnanometre heterodyne interferometric system with improved phase sensitivity using a three-longitudinal-mode He-Ne laser. *Meas. Sci. Technol.*, 12: 157-162.

Yokoyama, S., T. Yokoyama and T. Araki, 2005. High-speed subnanometre interferometry using an improved three-mode heterodyne interferometer. *Meas. Sci. Technol.*, 16: 1841-1847.